Evaluation of the Backflashover Performance of a 150 kV Overhead Transmission Line Considering Frequency- and Current-Dependent Effects of Tower Grounding Systems

Zacharias G. Datsios ⓘ, *Member, IEEE*, Erika Stracqualursi ⓘ, *Member, IEEE*,
Diamantis G. Patsalis ⓘ, *Student Member, IEEE*, Rodolfo Araneo ⓘ, *Senior Member, IEEE*,
Pantelis N. Mikropoulos ⓘ, *Senior Member, IEEE*, and Thomas E. Tsovilis ⓘ, *Senior Member, IEEE*

Abstract—The influence of the frequency- and current-dependent response of tower grounding systems on evaluating the backflashover performance of a typical 150 kV overhead transmission line is investigated in this study. This is achieved by adopting different tower grounding system modeling approaches in ATP-EMTP simulations: 1) a simple resistor (constant resistance value), 2) the frequency-dependent (FD) grounding system response with constant electrical properties of soil, 3) the FD response with FD soil properties, and 4) a soil ionization model. FD responses for concentrated and extended tower grounding systems are obtained via a hybrid method based on electromagnetic field analysis and circuit theory. Backflashover rate, *BFR*, is estimated by obtaining the minimum backflashover current of the line through ATP-EMTP simulations. Different first return-stroke currents of negative downward lightning flashes are employed in simulations, namely CIGRE WG 33.01 waveforms considering the statistical distributions of their parameters, recorded waveforms, and approximations of the latter with the CIGRE waveform. The impact of the lightning peak current distribution on *BFR* results is assessed. The evaluated backflashover performance is affected considerably by the FD tower grounding system response for extended systems, whereas by soil ionization for concentrated systems; for the latter, FD effects influence *BFR* mainly for low soil resistivity values.

I. INTRODUCTION

THE evaluation of lightning overvoltages stressing the insulation of power systems is important for insulation coordination and surge protection studies. It requires the accurate prediction of the response of grounding systems during the flow of lightning currents to the ground. This response is frequency- and current-dependent, as it is dominated by the frequency dependence of the behavior of ground electrodes and soil electrical properties, as well as by soil ionization. The latter phenomenon refers to electrical discharges developing in areas of high electric field strength in the ground, leading to a reduction of the impulse ground impedance. Several factors affect these phenomena, including soil properties, geometry and dimensions of the ground electrodes, as well as lightning current waveform, amplitude, and polarity.

Generally, grounding system modeling for fast-front transient studies is a formidable task. This is due to the complexity of the related phenomena, the varying conditions and non-uniformity of soil (as a complex multiphase particulate material) together with grounding system geometry and dimensions effects. Hence, investigations related to grounding system impulse behavior and modeling still attract considerable interest [1], [2], [3], [4], [5], [6], [7], [8], [9], [10], [11], [12], [13], [14], [15], [16]. Despite recent advances, existing modeling approaches may predict notably different grounding system responses introducing uncertainty in simulation results associated with lightning transient studies. This also applies for the evaluation of the backflashover performance of overhead transmission lines (OHTLs). In this case, the modeling approach adopted for the grounding systems of transmission towers is crucial, as the predicted grounding system response determines the computed overvoltages across OHTLs insulation due to direct lightning strikes to towers and overhead ground wires (OHGWs). Hence, it affects the computation of the minimum (critical) lightning current causing backflashover, I_{BF}, and thus, of the backflashover rate, *BFR*.

Zacharias G. Datsios, Diamantis G. Patsalis, Pantelis N. Mikropoulos, and Thomas E. Tsovilis are with the High Voltage Laboratory, School of Electrical & Computer Engineering, Aristotle University of Thessaloniki, 541 24 Thessaloniki, Greece (e-mail: zdatsios@auth.gr; dpatsalis@ece.auth.gr; pnm@eng.auth.gr; tsovilis@auth.gr).

Erika Stracqualursi and Rodolfo Araneo are with the Department of Astronautical, Electrical and Energy Engineering, University of Rome "Sapienza", 00185 Rome, Italy (e-mail: erika.stracqualursi@uniroma1.it; rodolfo.araneo@uniroma1.it).

Digital Object Identifier 10.1109/TIA.2023.3338132

Considering the above, there could be uncertainty in I_{BF} and *BFR* estimates due to tower grounding system modeling.

This study investigates the influence of frequency- and current-dependent effects, which dominate the lightning transient response of grounding systems, on the evaluation of the backflashover performance of a typical 150 kV double-circuit OHTL. This is achieved by adopting different tower grounding system modeling approaches in ATP-EMTP simulations [17], [18], which are performed for the estimation of I_{BF}; the latter is then used for computing *BFR*. The concentrated and extended grounding systems constructed in practice for the 150 kV towers are considered. Frequency-dependent (FD) grounding system responses are obtained via a hybrid method [19] based on electromagnetic field analysis and circuit theory, using both constant and FD soil electrical properties while taking the low-frequency (LF) soil resistivity, ρ_{LF}, as an influencing parameter. The obtained responses are introduced in ATP-EMTP simulations with the aid of vector fitting [20], [21], [22]. A soil ionization model is also applied in ATP-EMTP simulations. A preliminary investigation has been conducted in [1].

Even though there are relevant studies in the literature [23], [24], [25], [26] investigating the influence of tower grounding system modeling on assessing overvoltages and *BFR* of overhead lines, the effects of frequency- and current-dependent response of tower grounding systems on *BFR* are for the first time assessed using a *BFR* estimation methodology that considers solely the rate of direct strikes to OHTLs with currents exceeding I_{BF}, as introduced in [27]. This, together with a validated EMTP modeling approach of the investigated system (Section III), allows for evaluating *BFR* in an accurate manner. In addition, different lightning peak current distributions are used in *BFR* estimation; this enables generalization of conclusions, applying to different geographical regions worldwide. Finally, for the first time, recorded first return-stroke current waveforms of negative downward lightning flashes are used in simulations accounting also for frequency- and current-dependent effects of grounding systems; in the highly relevant investigation of [28], tower grounding systems are represented by resistors. Hence, the impact of approximating recorded waveforms with the waveform proposed by CIGRE WG 33.01 [29], [30] is evaluated in this work using more sophisticated modeling approaches.

II. 150 kV OVERHEAD TRANSMISSION LINE CHARACTERISTICS

A typical 150 kV double-circuit OHTL and the concentrated and extended grounding systems constructed in practice for the transmission towers are modeled in this work. Fig. 1 presents the data required for developing the OHTL model in ATP-EMTP [17], [18]. It is noted that such double-circuit OHTLs are adopted worldwide with little differences.

Fig. 2 shows the geometry and dimensions of the grounding systems. The commonly employed concentrated system (Fig. 2(a)) comprises four ground rods (length: 2 m, diameter: 20 mm, installation depth: 3 m). In areas of high soil resistivity, when a power-frequency ground resistance, R_g, higher than 20 Ω is measured for the concentrated system, the extended
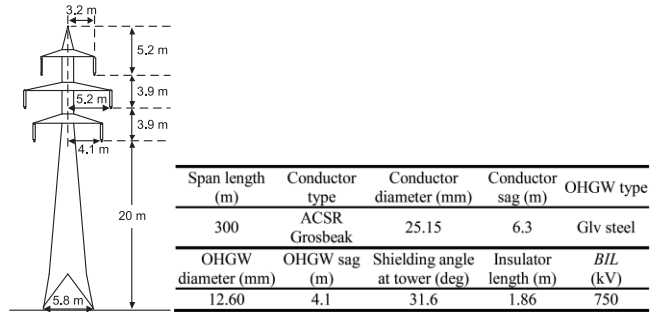
Fig. 1. Typical transmission tower (not in scale) of the studied 150 kV overhead line; inset table: Line characteristics.
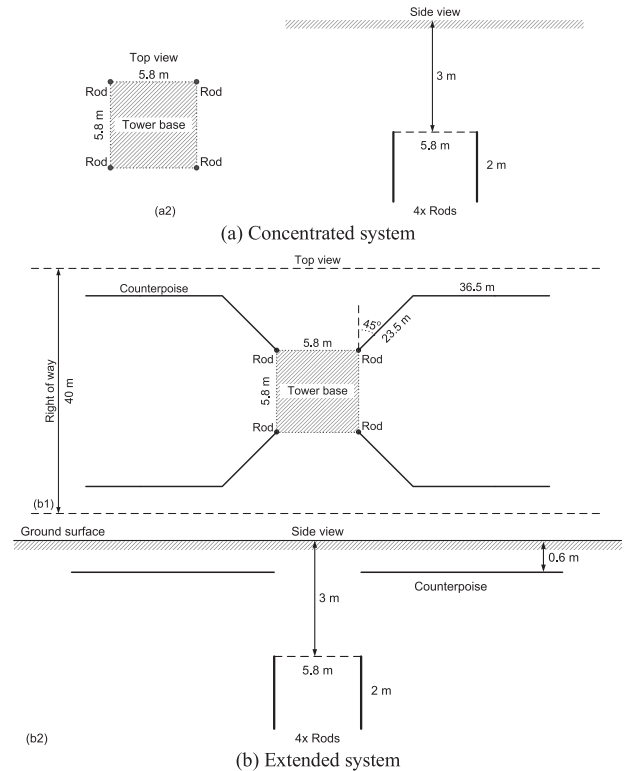
Fig. 2. (a) Concentrated and (b) extended grounding systems (not in scale) constructed in practice for the typical 150 kV transmission tower of Fig. 1.

system shown in Fig. 2(b) is constructed. The extended system consists of the four rods and four counterpoise wires, i.e, horizontal ground electrodes (length: 60 m, diameter: 10 mm, installation depth: 0.6 m). Nevertheless, the response of the concentrated system is evaluated in this work for $R_g > 20$ Ω as well, since installation of counterpoise wires is often not possible due to terrain constraints.

III. ATP-EMTP MODELING AND SIMULATION CASES

A. General Settings

The modeling approach of [27], [28], [31], [32] was adapted accordingly and used in this work for the 150 kV OHTL (Section II). A summary of the employed models and techniques

Line component	Modeling description
Overhead line	12 JMarti models [33]: 　10 spans, 2 long terminations to avoid reflections Superbundle configuration: ABC-ABC (A: upper conductor) Soil resistivity, ρ_{LF}: equal to the value used for tower grounding system modeling (Table II)
Towers	Lossless frequency-independent line Surge impedance: 167 Ω (conical tower [34]) Surge velocity: 85% of the speed of light [35]
Cap-and-pin insulator string negative flashover	CIGRE [29] leader development model Predischarge current included in simulations [36], [37]
Tower grounding systems	As from Subsection III.B, for both concentrated and extended grounding systems of Fig. 2: 　1) simple resistor with a resistance value equal to the power-frequency ground resistance, R_g [35] (R_g values given in Table II) 　2) frequency-dependent (FD) response of the grounding system; constant electrical properties of soil (ρ_{LF} and ε_{r10MHz} values given in Table II) 　3) FD response of the grounding system with FD soil properties (Longmire and Smith model [38], ρ_{DC} values listed in Table II) Solely for the concentrated grounding system of Fig. 2a: 　4) CIGRE soil ionization model [29] (R_g values in Table II) Simulation cases: Subsection III.C
Power-frequency voltage	Cosine function 12 phase angle values (0°-330°)
Negative lightning return-stroke	Current source in parallel to a lightning channel equivalent impedance of 400 Ω [32] (Norton equivalent) CIGRE [29], [30] and recorded [39], [40] lightning current waveforms for the simulation cases in Table III Recorded waveforms: 　– digitization time interval: variable. It reproduces main features of the waveforms 　– linear interpolation 　– implemented via MODELS language [41], [42] using an external pointlist function Lightning strikes the tower located in the middle of the line section (symmetrical line model)
Time step and total simulation time	1 ns and 30-50 μs, respectively

A short discussion on the validity of the adopted ATP-EMTP modeling approach for the computation of lightning overvoltages and critical flashover currents of overhead lines has been made in Appendix B of [28]. This approach has been validated successfully against the field measurements of lightning overvoltages arising at a 275 kV OHTL reported in [43].

is presented in Table I. The grounding system modeling approaches listed in Table I are described in the following subsection; the simulation cases are detailed in Subsection III-C.

B. Tower Grounding System Modeling

The tower grounding system modeling approaches adopted in this study are suitable for time-domain simulations with ATP-EMTP. These are summarized in Table I and are described in what follows.

1) Resistor With a Constant Resistance Value Equal to the Power-Frequency Tower Ground Resistance: This is a simplified method, according to which the tower grounding system is

represented by a single resistor with a resistance value equal to the power-frequency tower ground resistance, R_g. The adoption of R_g in computations and simulations has been a common approach for a long time [35] and is frequently encountered in literature. In addition to its simplicity, this is because R_g is commonly measured for most OHTLs. It also yields conservative lightning overvoltages and critical backflashover currents for concentrated grounding systems. This is also the case for extended systems when their length is shorter than the effective, that is, their impulse ground impedance is lower than R_g, as discussed in more detail in Subsection II-C of [27]. The use of R_g is further investigated in this work.

2) Frequency-Dependent Behavior of Tower Grounding Systems: The FD response of the concentrated and extended tower grounding systems of Fig. 2 is obtained by a numerical code [19] implementing the hybrid method [44], which is based on electromagnetic field analysis and circuit theory. Both constant and FD electrical properties of soil were employed, the latter via the Longmire and Smith [38] FD soil model. For computing the frequency spectra of the complex ground impedance, that is, the output of the hybrid method code, the ground electrodes are represented by thin, electrically short branches, interconnected by nodes. Standard nodal analysis is applied to solve the problem. Actually, a matrix of nodal admittances is constructed and its elements are determined by solving the associated electromagnetic problem, which requires the computation of the Green functions for the scalar electric potential and dyadic magnetic potential in layered lossy media. The frequency dependence of soil electrical properties is easily accounted for; soil resistivity, $\rho(f)$, and relative permittivity, $\varepsilon_r(f)$, as predicted by the FD soil model, are used as inputs for the hybrid method to obtain the response of the grounding system at each frequency, f. The harmonic ground impedance, $Z_g(f)$, is defined as:

$$Z_g(f) = V(f)/I(f) \qquad (1)$$

where $V(f)$ is the voltage at the nodes of the grounding system where the lightning current is expected to be injected (these nodes are assigned the same voltage value), and $I(f)$ is the total current flowing to these nodes. The results of the hybrid method code have been validated beforehand in [1] against literature data for horizontal and vertical ground electrodes.

The computed FD responses are introduced in ATP-EMTP with the aid of vector fitting [20], [21], [22]. A Netlist file (equivalent lumped circuit) is produced for each response and a user-specified object is employed in ATPDraw [45] for each tower to import the Netlist file with an $INCLUDE statement. Before backflashover simulations, the frequency scan option of ATP-EMTP is utilized to verify the correspondence of the FD response of the Netlist file with the original response obtained via the hybrid method code.

It is noted that a code has also been developed in MODELS language [41], [42] for importing an FD response approximated by a rational function in the polynomial form. This alternative method yields equivalent results with the Netlist file and user-specified object approach; however, it requires a considerably longer simulation time as it is based on a circuit-type component

TABLE II
SOIL ELECTRICAL PROPERTIES AND TOWER GROUND RESISTANCES USED IN SIMULATIONS

		Concentrated system (Fig. 2a); R_g=0.1169·ρ_{LF}							Extended system (Fig. 2b); R_g=0.010922·ρ_{LF}			
R_g	(Ω)	7	10	25	50	100	150	200	7	10	25	50
ρ_{100Hz}=ρ_{LF}	(Ωm)	59.9	85.5	213.9	427.7	855.4	1283.1	1710.8	640.9	915.3	2288.8	4577.6
ρ_{DC}	(Ωm)	62.4	89.5	227.2	460.0	933.5	1416.0	1906.0	695.0	1001.0	2576.0	5284.0
ε_{r10MHz}	–	23.9	21.9	16.9	14.4	12.9	12.0	11.3	13.5	12.7	10.7	9.4

(Thévenin type-94). Hence, the Netlist file and user-specified object approach was used in this work.

3) CIGRE Soil Ionization Model [29]: As summarized in [46], [47], a large number of soil ionization models has been proposed for concentrated grounding systems. These predict the instantaneous impulse ground impedance, $R(I)$, which is lower than R_g due to the occurrence of electrical discharges in the ground. The most popular soil ionization model, introduced by CIGRE WG 33.01 [29], is adopted in this paper for the concentrated tower grounding system of Fig. 2(a).

$$R(I) = R_g/\sqrt{1 + I/I_g} \qquad (2)$$

In (2), $R(I)$ and R_g are in Ω, I (kA) is the instantaneous current flowing to the ground, I_g (kA) is calculated by (3) and it is defined as the critical current that is necessary to yield an $R(I)$ value considerably lower than R_g.

$$I_g = E_0 \cdot \rho_{LF}/\left(2\pi \cdot R_g^2\right) \qquad (3)$$

In (3), E_0 (kV/m) is the critical soil ionization gradient and ρ_{LF} (Ωm) is the LF soil resistivity. A value of 400 kV/m is used in this work for E_0, as proposed by CIGRE [29]. Note that the CIGRE soil ionization model was introduced in ATP-EMTP simulations via the TGIR object [46]; the latter has been developed using MODELS language of ATP-EMTP and implements several soil ionization models for concentrated grounding systems.

C. Simulation Cases

Table II presents the selected values of the soil electrical properties (LF soil resistivity, ρ_{LF}, DC soil resistivity, ρ_{DC}, and real relative permittivity at 10 MHz, ε_{r10MHz}) together with the associated power-frequency ground resistance, R_g. The following input parameters are required for each modeling approach:
1) R_g for the resistor modeling approach.
2) ρ_{LF} and ε_{r10MHz} for the FD response with constant soil properties.
3) ρ_{DC} for the FD response with FD soil properties. The variation of soil resistivity, $\rho(f)$, and relative permittivity, $\varepsilon_r(f)$, with frequency, f, is predicted by the Longmire and Smith FD soil model [38] considering the relative electrical permittivity at infinite frequency ($\varepsilon_{r\infty} = 5$ [38]) and ρ_{DC}; the latter is selected to obtain the ρ_{100Hz} values of Table II when using the Longmire and Smith model at $f = 100$ Hz.
4) R_g and ρ_{LF} for the CIGRE soil ionization model.

It is noted that initially the R_g values were selected; afterwards the corresponding ρ_{LF}, ρ_{DC}, and ε_{r10MHz} values were

TABLE III
FIRST RETURN-STROKE CURRENT WAVEFORMS OF NEGATIVE DOWNWARD LIGHTNING FLASHES; ADAPTED FROM [28]

Case	Waveform	Parameters	Information
W2 [39], W3 [40]	Recorded	Fig. 3	
W2, W3 approximation	CIGRE	Approximation of the recorded waveforms (Fig. 3)	
Best-case scenario		$(t_{d30,5\%}, S_{m,95\%}, t_{h,95\%})$	Highest critical current
Worst-case scenario	CIGRE	$(t_{d30,95\%}, S_{m,5\%}, t_{h,5\%})$	Lowest critical current
Median parameters		$(t_{d30,50\%}, S_{m,50\%}, t_{h,50\%})$	Commonly used in lightning performance studies

t_{d30}: front time, S_m: maximum steepness, and t_h: time to half value (definitions according to CIGRE [29], [30]). Percentages in subscripts denote cases exceeding this parameter value as given in Table IV of [28] where the statistical distributions proposed by CIGRE [29] have been adopted. t_{d30} and S_m values depend on the lightning peak current.
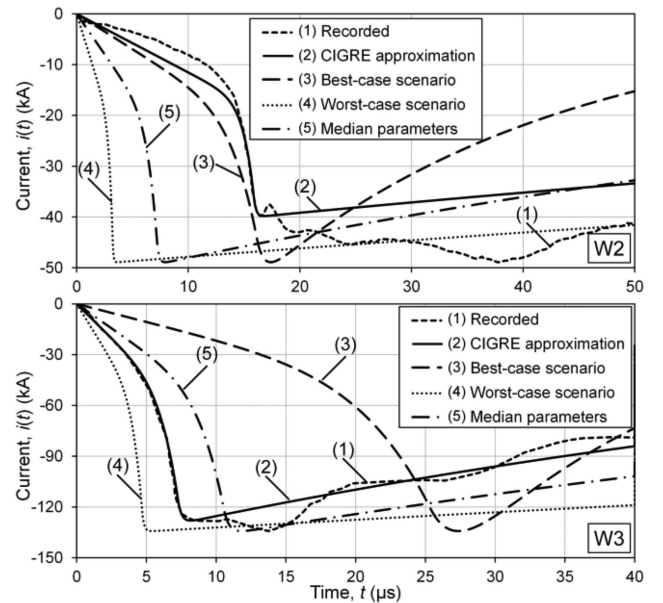

Fig. 3. Waveforms of negative first return-stroke currents employed in simulations.

determined (ρ_{LF} via the hybrid method code and ρ_{DC}, ε_{r10MHz} by using the Longmire and Smith model).

Table III details the first return-stroke current waveforms of negative downward lightning flashes employed in simulations. These comprise two recorded waveforms (W2 and W3 in Fig. 3 with characteristics listed in Table IV; waveform naming in accordance with [28]) differing in waveshape parameters, the corresponding CIGRE waveform approximations (Fig. 3), as well as CIGRE waveforms considering the statistical distributions of waveform parameters. More specifically, three cases are employed in simulations (Table III): the median values, commonly used in lightning performance studies for estimating the

TABLE IV
WAVEFORM PARAMETERS OF THE RECORDED FIRST RETURN-STROKE
CURRENTS OF NEGATIVE DOWNWARD LIGHTNING FLASHES SHOWN IN FIG. 3

	Waveform		I_I (kA)	I_F (kA)	t_{d30} (µs)	S_m (kA/µs)	t_h (µs)
W2	Berger Fig. 15 of [39]	no. 6236	39.8	48.9	5.5	25.5	139.4
W3	Narita et al. Fig. 5 of [40]		128.2	134.2	5.3	55.0	52.5

Definitions of waveform parameters according to CIGRE [29], [30].
I_I: initial (first) lightning current peak, I_F: final (second) lightning current peak
(usually $I_F > I_I$), t_{d30}: front time, S_m: maximum steepness, and t_h: time to half value.
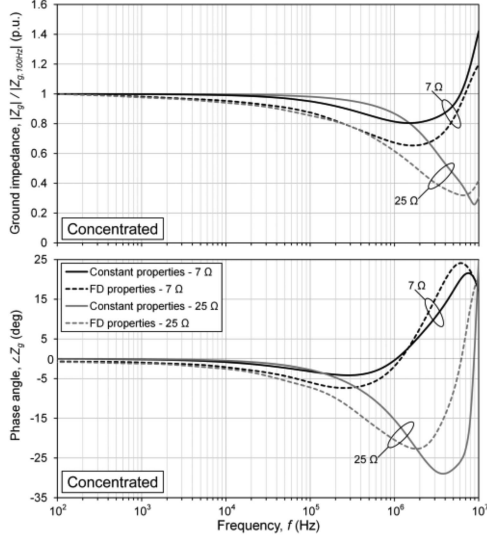

Fig. 4. FD responses of the concentrated grounding system (Fig. 2(a)) with constant and FD soil properties corresponding to $R_g = 7\ \Omega$ and 25 Ω (Table II).

lightning performance of OHTLs, and the best- and worst-case scenarios for the critical backflashover current. The best-case (worst-case) scenario corresponds to the highest (lowest) I_{BF} value, long (short) wavefront, low (high) steepness, and short (long) wavetail.

IV. FREQUENCY-DEPENDENT RESPONSES OF THE CONCENTRATED AND EXTENDED GROUNDING SYSTEMS

Simulations of the tower grounding systems of Fig. 2 have been conducted using the hybrid method to obtain their FD responses with both constant and FD soil electrical properties (Subsection III-B-2). The R_g cases of Table II have been investigated by using the corresponding values of ρ_{LF} and ρ_{DC} (Table II) in simulations, obtaining thus an LF ground impedance $Z_{g,LF} \approx R_g$.

Figs. 4 and 5 depict typical results of the hybrid method for the concentrated (Fig. 2(a)) and extended (Fig. 2(b)) tower grounding systems, respectively. These refer to the magnitude and argument of Z_g for the cases of $R_g = 7\ \Omega$ and 25 Ω. It is noted that the magnitude of Z_g has been normalized with its value at 100 Hz, $|Z_{g,100Hz}|$. From Figs. 4 and 5, it is evident that for relatively low frequencies $Z_g \approx R_g$ and the grounding system behavior is resistive ($\angle Z_g \approx 0^\circ$). However, for higher frequencies, the reactive component of Z_g is significant.
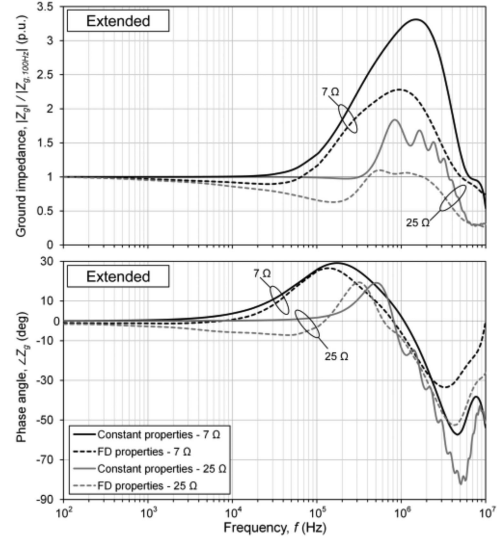

Fig. 5. FD responses of the extended grounding system (Fig. 2(b)) with constant and FD soil properties corresponding to $R_g = 7\ \Omega$ and 25 Ω (Table II).

The frequency responses of the concentrated and extended grounding systems in Figs. 4 and 5 differ for the same R_g value due to their characteristic dimension. The length of each rod (2 m) is shorter or of the same order of magnitude of the minimum wavelength λ_{min} in the frequency range of interest for the simulated soil properties. Thus, the propagation along the vertical rods is not important. On the other hand, propagation along the counterpoise wires is relevant due to their long length (60 m).

When constant soil electrical properties are employed in simulations, the concentrated grounding system exhibits a capacitive behavior above a frequency value, that is, $|Z_g(f)| < R_g$ (Fig. 4), whereas the behavior of the extended system becomes inductive (Fig. 5). This means that the performance of the extended system deteriorates as the frequency increases ($|Z_g(f)| > R_g$).

When the frequency dependence of the electrical properties of soil is taken into account, a capacitive behavior is observed above a relatively low frequency limit for both concentrated and extended configurations (Figs. 4 and 5). This is due to the high permittivity values predicted by Longmire and Smith soil model [38]. The latter also predicts a considerable reduction of the resistivity of soil with increasing frequency, leading to a reduction of the ground impedance magnitude.

V. ATP-EMTP SIMULATION RESULTS AND DISCUSSION

A. Lightning Overvoltages

1) Concentrated Grounding System: Fig. 6 shows the lightning overvoltages stressing the insulators of the 150 kV OHTL (Fig. 1) computed with ATP-EMTP for the investigated modeling approaches (Subsection III-B) of the concentrated tower grounding system (Fig. 2(a)); each subfigure corresponds to an R_g value (Table II). The presented overvoltages refer to the insulator stressed the most (at the positive peak of the phase conductor AC voltage when lightning strikes). They were
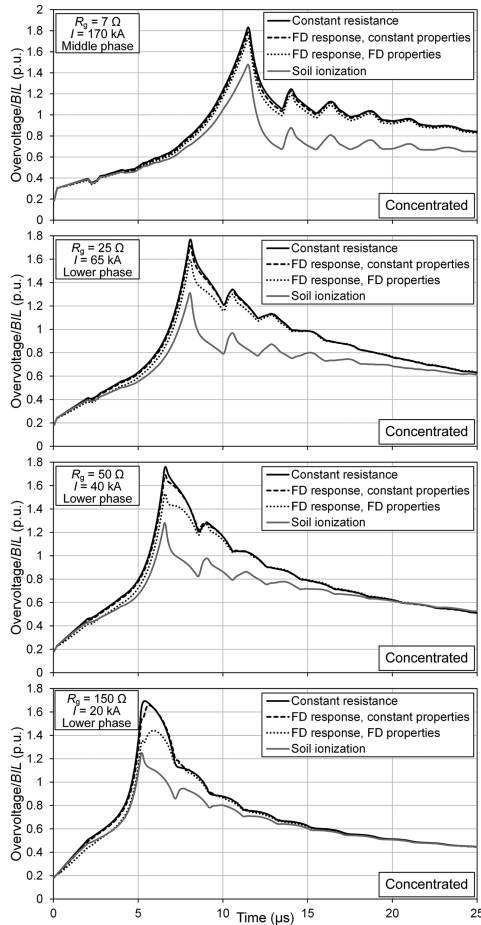
Fig. 6.   Normalized lightning overvoltages (withstand cases) stressing the insulation of the 150 kV overhead line of Fig. 1. Grounding system: Concentrated (Fig. 2(a)); $R_g = 7, 25, 50, 150\ \Omega$. CIGRE waveform parameters: Median values.
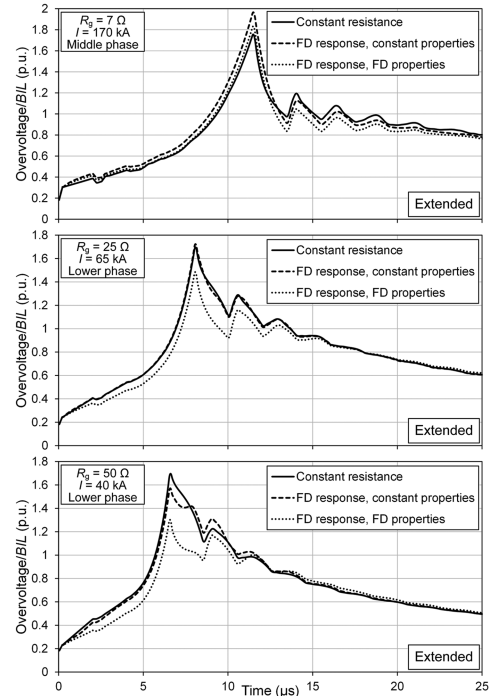

Fig. 7.   Normalized lightning overvoltages (withstand cases) stressing the insulation of the 150 kV overhead line of Fig. 1. Grounding system: Extended (Fig. 2(b)); $R_g = 7, 25, 50\ \Omega$. CIGRE waveform parameters: Median values.

obtained for lightning peak currents slightly lower than the lowest backflashover current of each case. Note that overvoltages are normalized against the Basic Insulation Level, *BIL*, of the line (750 kV).

From Fig. 6, it can be observed that the highest overvoltages are obtained using the R_g approach. These are reduced when considering the FD responses. A small reduction is obtained for the case of constant electrical properties of soil. The corresponding reduction for the FD soil properties is larger and is enhanced for higher R_g values. This is in line with the FD responses of Fig. 4. It is important that the overvoltage waveforms for these three cases converge at the wavetail, however, within the flashover times. When considering soil ionization in simulations, a significant reduction of the lightning overvoltages is observed irrespectively of the R_g value. The convergence of the overvoltage waveforms associated with soil ionization with those of previous cases occurs much later and beyond probable flashover times for relatively low R_g.

The results of Fig. 6, as well as those for the extended tower grounding system presented in Fig. 7, indicate that the modeling approach for the grounding system affects I_{BF}. This will be discussed in Subsection V-B. From Fig. 6 for the concentrated

grounding system, it can be deduced that a higher I_{BF} is expected for the cases of the FD responses and soil ionization.

2) Extended Grounding System: Similarly to Fig. 6, the lightning overvoltages for the extended tower grounding system are depicted in Fig. 7. For relatively low R_g values, it can be seen that, the instantaneous overvoltages may be higher when considering the FD responses in simulations due to the inductive behavior of the grounding system (Fig. 5). Hence, a lower I_{BF} and a higher *BFR* may be obtained. For high R_g values, the FD responses yield lower overvoltages than the use of R_g in simulations, as capacitive effects dominate. These observations depend also on the adopted soil modeling approach (constant or FD) due to the considerable reduction of soil resistivity with increasing frequency for FD soil properties; this is very important for high ρ_{LF} values. In addition, by comparing Figs. 6 and 7, it can be observed that the FD effects on the computed overvoltages are more pronounced for the extended grounding system; this is also the case for the minimum backflashover current dealt with in the next subsection.

B. Critical Backflashover Current

1) Concentrated Grounding System: Fig. 8 shows the variation of I_{BF} with R_g for the concentrated grounding system of Fig. 2(a) and the investigated modeling approaches of Subsection III-B for the 150 kV OHTL. The threshold (lowest) I_{BFthr} is depicted in Fig. 8. This is typically linked to backflashover at the lower phase insulator for AC voltage phase angle of 240° (positive AC peak of the lower phase) except for the cases with $R_g \leq 10\ \Omega$ for which the critical phase angle could be 120° and

Fig. 8. Threshold backflashover current, I_{BFthr}, of the 150 kV overhead line (Fig. 1) versus power-frequency tower ground resistance, R_g. Grounding system: Concentrated (Fig. 2(a)). CIGRE waveform parameters: Median values.
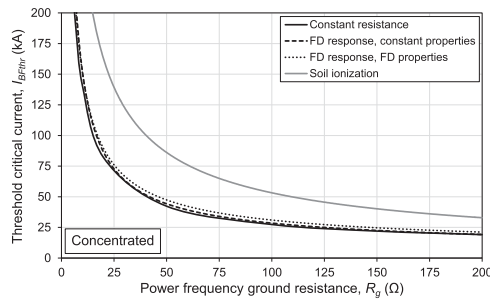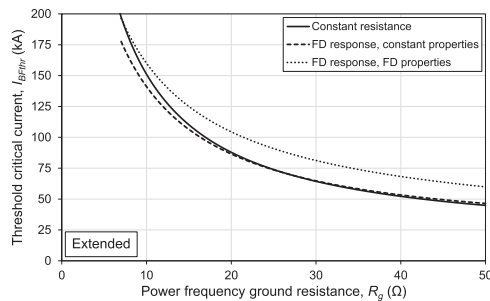

Fig. 9. Threshold backflashover current, I_{BFthr}, of the 150 kV overhead line (Fig. 1) versus power-frequency tower ground resistance, R_g. Grounding system: Extended (Fig. 2(b)). CIGRE waveform parameters: Median values.

the middle insulator may flashover instead. It was found that this depends on the lightning current waveform, the grounding system, and its modeling approach. The I_{BF} values of Fig. 8 were obtained for the CIGRE waveform with median parameters, as these are commonly used for the evaluation of the backflashover performance of OHTLs.

From Fig. 8, it can be observed that the differences in I_{BFthr} are minor when using in simulations R_g and the FD response with constant soil properties for the concentrated grounding system. The FD case yields 1.5% to 3% higher I_{BFthr}, increasing with decreasing R_g. Greater differences are obtained with FD soil properties (8% to 16% higher I_{BFthr} values, augmenting with increasing R_g), in line with the overvoltage results of Fig. 6. From Fig. 8 it is also evident that the effects of soil ionization on I_{BFthr} are remarkable (from 75% up to >100% higher I_{BFthr} values with respect to those computed with a constant R_g). This is due to the sizable reduction of the instantaneous impulse ground impedance predicted by this model.

2) Extended Grounding System: Fig. 9 depicts the I_{BFthr} results for the extended grounding system of Fig. 2(b). Conservative I_{BFthr} values are obtained for the FD response with constant soil properties. For $R_g > 25 \ \Omega$, the representation of the grounding system with R_g yields practically the same I_{BFthr} values. When considering the FD soil properties, I_{BFthr} is generally higher for the investigated cases, due to lower instantaneous overvoltage values (Fig. 7).

The variation of I_{BF} with R_g was found to be comparable with that of Figs. 8 and 9 for all 12 investigated AC operating voltage

phase angle values (Table I). The obtained I_{BF} results for these 12 angles are used for the computation of *BFR* in Section VI.

C. Investigation on Recorded Lightning Current Waveforms and Their CIGRE Approximations

Simulations have also been conducted for the recorded and CIGRE lightning current waveforms of Table III and Fig. 3. This is an extension of the investigation presented recently in [28] where tower grounding systems were represented by resistors with resistance equal to R_g. Fig. 10 shows computed overvoltages at the lower insulator of the 150 kV OHTL for the grounding systems of Fig. 2 and the investigated modeling approaches (Subsection III-B). The overvoltages of Fig. 10 correspond to the W2 and W3 recorded waveforms and the best- and worst-case scenarios for I_{BF} (Subsection III-C). The overvoltages for the CIGRE approximation of the recorded waveforms have been omitted since their form is comparable to that of Figs. 6 and 7, which correspond to CIGRE waveforms with median parameter values. From Fig. 10, it is evident that the peak and the waveshape of the overvoltages vary remarkably among the investigated lightning current waveforms. The instantaneous values of the overvoltages obtained for the recorded lightning currents exhibit larger variations with time. Regarding the effects of the grounding system modeling, the observations made on the overvoltages for the concentrated (Fig. 6) and extended (Fig. 7) grounding systems in Subsection V-A still hold in general. It is important that the largest (smallest) differences among models are found for the worst-case (best-case) scenario lightning current. This is because the latter exhibits a short wavefront with high steepness, that is, a high frequency content resulting in more pronounced effects associated with the FD behavior of the grounding system; the opposite applies for the best-case scenario current.

Fig. 11 shows the I_{BFthr} values of the 150 kV OHTL for the evaluated lightning current waveforms (Table III and Fig. 3), grounding systems (Fig. 2), and their modeling approaches (Subsection III-B). The I_{BFthr} values for the CIGRE approximation are lower (3% to 21%) than those for the recorded waveforms. This effect, being more marked for the W2 waveform, is due to higher overvoltages for the CIGRE approximations, as their single peak corresponds to the first (lower) peak of the recorded waveforms (Fig. 3). Hence, when scaled up to the same maximum value (single peak for the CIGRE approximations and second peak for the recorded waveforms) the steepness of the CIGRE approximation waveforms is higher due to the shorter time to peak; this has been further discussed in [28]. The worst-case scenario yields indeed the most conservative I_{BFthr}, while, for W3 ($R_g = 10 \ \Omega$), the most optimistic values of I_{BFthr} are found for the best-case scenario. However, for W2, the recorded waveform results in the highest I_{BFthr}. Finally, when the median parameters are used in simulations, the computed I_{BFthr} is in the range defined by the values associated with the worst- and best-case scenarios, closer to the lower limit (worst-case).

From Fig. 11, it can be deduced that for the concentrated system the FD behavior of the grounding system generally does not influence the above discussion. On the contrary, current-dependent effects (soil ionization) enhance considerably the
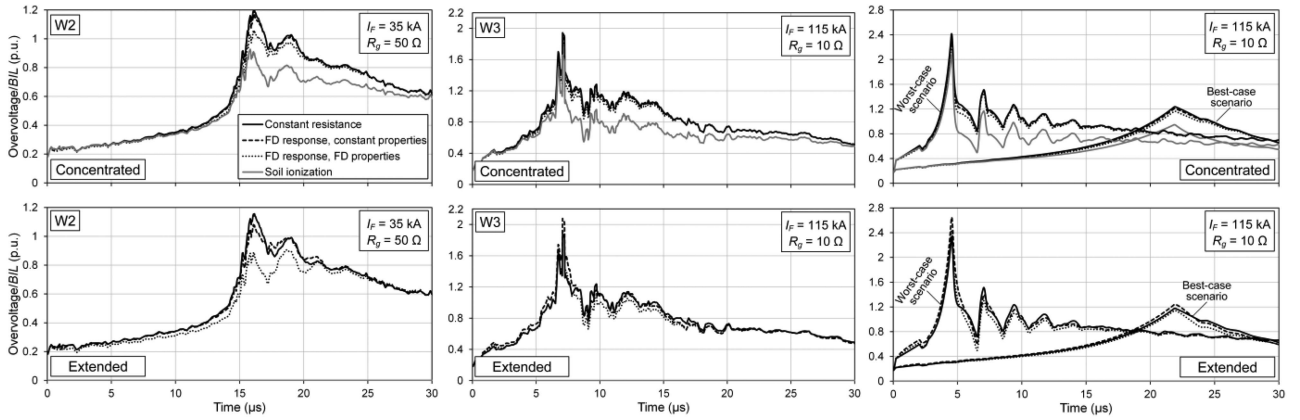
Fig. 10. Normalized lightning overvoltages (withstand cases) stressing the lower insulator of the 150 kV overhead line of Fig. 1 for the tower grounding systems of Fig. 2. Lightning currents: Recorded waveforms (W2, W3) and CIGRE waveforms for the best- and worst-case scenarios (Table III and Fig. 3).
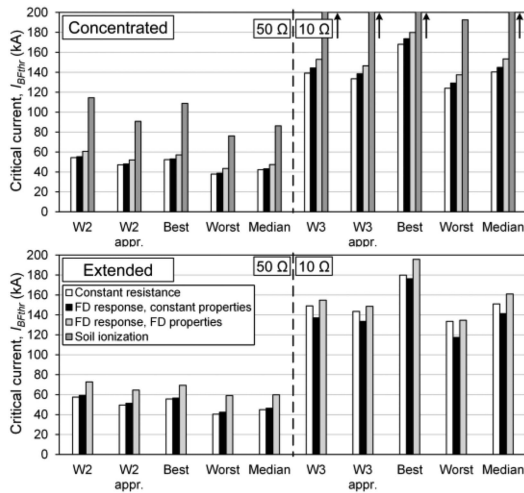

Fig. 11. Threshold backflashover current, I_{BFthr}, of the 150 kV overhead line (Fig. 1) for the recorded (W2 and W3) and the CIGRE waveforms of Table III and Fig. 3. Arrows denote values higher than 200 kA. R_g values: 10 and 50 Ω.

differences on I_{BFthr} among waveforms. For the extended system, the FD effects lessen or enhance differences to a certain extent depending on the FD response of the grounding system. Differences decrease (increase) when a capacitive (inductive) behavior prevails. This can be attributed to the counterpoise wires being long enough to make propagation effects relevant. It is also noted that the same R_g corresponds to higher soil resistivity for the extended (than the concentrated) system (Table II), increasing the significance of using FD soil electrical properties. In light of the above, the results and conclusions of [28] on the effects of recorded lightning current waveforms and their CIGRE approximations on computed backflashover overvoltages and critical currents also apply for more sophisticated modeling of the tower grounding system than the simple use of R_g.

VI. EFFECTS ON BACKFLASHOVER RATE

The backflashover rate, *BFR*, of the 150 kV OHTL of Fig. 1 has been computed by employing lightning incidence computations, considering solely the rate of direct strikes to the line with currents exceeding I_{BF} according to [27]. The variation of the
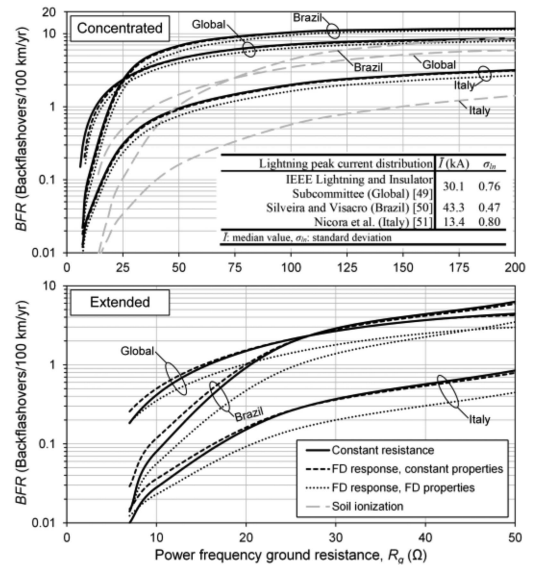

Fig. 12. Backflashover rate, *BFR*, of the 150 kV overhead line (Fig. 1) versus power-frequency tower ground resistance, R_g, of the grounding systems of Fig. 2, with lightning peak current distribution as parameter. *BFR* estimation methodology according to [27].

AC voltage has been considered, the ground flash density, N_g, was taken 1 flash/km²/yr, and the lightning attachment model of IEEE Std 1243 [48] was used. Three probability density functions of the lightning crest current distribution were applied [49], [50], [51], as they affect *BFR* more than the attachment models [52].

Fig. 12 shows the *BFR* as a function of R_g for the grounding systems of Fig. 2, the models of Subsection III-B, and the lightning current distributions of its inset table. When considering the "global" lightning current distribution [49] for the concentrated system (Fig. 2(a)), the *BFR* estimates obtained for soil ionization are lower from 30% up to >80%. When $R_g > 10$ Ω, the *BFR* accounting for the FD response with constant soil properties is almost equal (up to 1% lower) to the *BFR* obtained with the constant resistance; for $R_g < 10$ Ω differences are up to 10%. These are higher, from 7% to 23%, when FD soil properties are considered. Generally, the effect of grounding system modeling on *BFR* becomes higher for decreasing R_g due to the associated higher

I_{BF}. In fact, the lower probability of relatively high lightning currents enhances smaller differences in computed I_{BF} values.

As seen from Fig. 12, the FD response is more relevant for the extended grounding system (Fig. 2(b)). When constant soil properties are considered, the FD leads to conservative BFR values for $R_g < 25\,\Omega$ (up to 40% higher BFR than that of the R_g approach). For $R_g > 25\,\Omega$, conservative results are obtained for the R_g representation, although differences are minor. FD soil properties yield generally lower BFR (up to 33%).

The influence of the lightning peak current distribution on BFR is considerable, as seen from Fig. 12. The distribution from Brazil (tropical region) yields higher BFR than that from Italy (temperate region). The "global" distribution is in between for R_g values higher than ~25 Ω. However, for $R_g < 25\,\Omega$ (relatively high I_{BF}) the BFR estimated using the "global" distribution is the highest. This can be attributed to the relatively low σ_{ln} of the distribution from Brazil (inset table of Fig. 12). The impact of the lightning peak current distribution on the investigation of the effects of grounding system modeling on BFR is significant. The distributions affect considerably BFR computed by different grounding system models (Fig. 12). These differences are enhanced for the distribution from Italy, as well as from Brazil. However, for the latter distribution this is solely for high I_{BF} (low R_g); for low I_{BF}, differences in BFR become less pronounced.

The results of this study can be explained by the harmonic impedance, Z_g, and instantaneous impulse impedance of the tower grounding system. For the concentrated system, the FD behavior is capacitive due to its small dimensions for all R_g values. Thus, $|Z_g| < R_g$ for constant soil properties, leading to lower overvoltages, higher I_{BF}, and lower BFR. This is enhanced for FD soil properties due to the reduction of ρ with increasing frequency and higher ε_r values. Soil ionization extends the dimensions of the grounding system by surrounding it with conductive discharges, diminishing its impulse impedance. The behavior of the extended grounding system depends on ρ_{LF}, thus also on R_g. For low R_g values, the behavior at higher frequencies is inductive (Fig. 5) causing higher overvoltages. For higher ρ_{LF} the behavior becomes capacitive, and effects are similar to those of the concentrated system. This is enhanced by FD soil properties due to the reduction of ρ with frequency.

VII. CONCLUSION

The influence of frequency- and current-dependent grounding system effects on the evaluation of the backflashover performance of a typical 150 kV double-circuit OHTL has been investigated by adopting different tower grounding system modeling approaches in ATP-EMTP simulations. The minimum backflashover current, I_{BF}, and backflashover rate, BFR, have been computed for the actual concentrated and extended tower grounding systems of the OHTL; the LF soil resistivity, ρ_{LF}, thus also the power-frequency ground resistance, R_g, were taken as parameters. FD grounding system responses have been obtained via a hybrid method code for constant and FD soil electrical properties. A soil ionization model has been evaluated as well. Simulations have been performed for recorded lightning currents and their approximations via CIGRE waveforms, considering also the statistical distributions of their parameters.

For the concentrated grounding system, conservative BFR values were obtained for a constant resistance equal to R_g. The influence of the FD response is enhanced when FD soil properties are considered and for lower ρ_{LF} due to the lower probability of relatively high lightning currents. It is important that this is contrary to the fact that FD effects on overvoltages and I_{BF} are more pronounced for higher ρ_{LF}. The lowest BFR was obtained for the CIGRE soil ionization model, as it predicts a remarkable decrease of the impulse ground impedance, yielding notably lower overvoltages and higher I_{BF}. It can be concluded that for the concentrated grounding system the modeling effects on the evaluation of the backflashover performance of the OHTL are mainly current-dependent; FD effects are important for cases with $R_g \leq 25\,\Omega$.

The FD response is more relevant in general when considering the extended tower grounding system. The most conservative modeling approach depends on ρ_{LF}. The FD response should be considered for low ρ_{LF} values, as a constant resistance could yield unrealistic results (low BFR) by neglecting any inductive behavior. It is noted, however, that between FD soil electrical properties and constant resistance case, conservative results correspond to the latter.

The lightning peak current distribution affects considerably the differences in the estimated BFR among models. These differences are enhanced for a distribution from a temperate region. This is also the case for a distribution from a tropical region, however, solely for high I_{BF} (low R_g).

The CIGRE waveforms approximating recorded lightning currents yield conservative overvoltages and I_{BF} for all tower grounding system modeling approaches; higher differences were found for the soil ionization case. Actually, I_{BF} is up to 21% lower for the CIGRE approximation due to the higher wavefront steepness. When considering the statistical variation of the waveform parameters, it was found that the differences in computed overvoltages and I_{BF} among tower grounding system models are generally higher for waveforms with shorter and steeper wavefronts.

REFERENCES

[1] Z. G. Datsios, E. Stracqualursi, R. Araneo, P. N. Mikropoulos, and T. E. Tsovilis, "Estimation of the minimum backflashover current and backflashover rate of a 150 kV overhead transmission line: Frequency and current-dependent effects of grounding systems," in *Proc. IEEE Int. Conf. Environ. Elect. Eng. IEEE Ind. Commercial Power Syst. Europe*, 2022, pp. 1–6.

[2] J. He, R. Zeng, and B. Zhang, *Methodology and Technology for Power System Grounding*. Hoboken, NJ, USA: Wiley, 2013.

[3] F. Viola, P. Romano, and R. Miceli, "Finite-difference time-domain simulation of towers cascade under lightning surge conditions," *IEEE Trans. Ind. Appl.*, vol. 51, no. 6, pp. 4917–4923, Nov./Dec. 2015.

[4] J. He and B. Zhang, "Progress in lightning impulse characteristics of grounding electrodes with soil ionization," *IEEE Trans. Ind. Appl.*, vol. 51, no. 6, pp. 4924–4933, Nov./Dec. 2015.

[5] N. Harid, H. Griffiths, S. Mousa, D. Clark, S. Robson, and A. Haddad, "On the analysis of impulse test results on grounding systems," *IEEE Trans. Ind. Appl.*, vol. 51, no. 6, pp. 5324–5334, Nov./Dec. 2015.

[6] F. Koehler and J. Swingler, "Practical model for tower earthing systems in lightning simulations," *Elect. Power Syst. Res.*, vol. 158, pp. 306–314, May 2018.

[7] O. Kherif, S. Chiheb, M. Teguar, A. Mekhaldi, and N. Harid, "Time domain modeling of grounding systems' impulse response incorporating nonlinear and frequency-dependent aspects," *IEEE Trans. Electromagn. Compat.*, vol. 60, no. 4, pp. 907–916, Aug. 2018.

[8] S. Visacro, "The use of the impulse impedance as a concise representation of grounding electrodes in lightning protection applications," *IEEE Trans. Electromagn. Compat.*, vol. 60, no. 5, pp. 1602–1605, Oct. 2018.

[9] D. Luo, W. Sima, T. Yuan, P. Sun, W. Chen, and J. Wang, "Influence factor analysis and parameter calculation of soil discharge and recovery characteristics under successive impulse currents," *IEEE Trans. Power Del.*, vol. 34, no. 2, pp. 514–523, Apr. 2019.

[10] B. Salarieh, H. M. J. De Silva, and B. Kordi, "Electromagnetic transient modeling of grounding electrodes buried in frequency dependent soil with variable water content," *Elect. Power Syst. Res.*, vol. 189, Dec. 2020, Art. no. 106595.

[11] C. Wang, X. Liang, E. P. Adajar, and P. Loewen, "Investigation of seasonal variations of tower footing impedance in transmission line grounding systems," *IEEE Trans. Ind. Appl.*, vol. 57, no. 3, pp. 2274–2284, May/Jun. 2021.

[12] P. Ranjan, G. Parvathi, R. Sarathi, R. G. Robinson, N. Harid, and H. Griffiths, "Influence of water, acid rain and bentonite on ionization characteristics of sand under lightning impulse voltage," *IEEE Trans. Dielectrics Elect. Insul.*, vol. 28, no. 3, pp. 897–905, Jun. 2021.

[13] A. R. J. de Araújo et al., "Computation of ground potential rise and grounding impedance of simple arrangement of electrodes buried in frequency-dependent stratified soil," *Elect. Power Syst. Res.*, vol. 198, Sep. 2021, Art. no. 107364.

[14] Z. G. Datsios et al., "Experimental investigation of the lightning impulse behavior of wet sandy soil," *IEEE Trans. Ind. Appl.*, vol. 58, no. 1, pp. 212–223, Jan./Feb. 2022.

[15] L. Grcev, "Simple formulas for impulse characteristics of vertical and horizontal ground electrodes," *IEEE Trans. Power Del.*, vol. 37, no. 1, pp. 40–49, Feb. 2022.

[16] R. Alipio, A. de Conti, F. Vasconcellos, F. Moreira, N. Duarte, and J. Marti, "Tower-foot grounding model for EMT programs based on transmission line theory and Marti's model," *Elect. Power Syst. Res.*, vol. 223, Oct. 2023, Art. no. 109584.

[17] Canadian-American EMTP Users Group, *ATP Rule Book*, 1997.

[18] H. W. Dommel, *Electro-Magnetic Transients Program (EMTP) Theory Book*. Portland, OR, USA: Bonneville Power Admin., 1986.

[19] E. Stracqualursi and R. Araneo, "Transient impedance of grounding grids with different soil models," in *Proc. IEEE Int. Conf. Environ. Elect. Eng. IEEE Ind. Commercial Power Syst. Europe*, 2021, pp. 1–6.

[20] B. Gustavsen and A. Semlyen, "Rational approximation of frequency domain responses by vector fitting," *IEEE Trans. Power Del.*, vol. 14, no. 3, pp. 1052–1061, Jul. 1999.

[21] B. Gustavsen, "Improving the pole relocating properties of vector fitting," *IEEE Trans. Power Del.*, vol. 21, no. 3, pp. 1587–1592, Jul. 2006.

[22] D. Deschrijver, M. Mrozowski, T. Dhaene, and D. de Zutter, "Macro-modeling of multiport systems using a fast implementation of the vector fitting method," *IEEE Microw. Wireless Compon. Lett.*, vol. 18, no. 6, pp. 383–385, Jun. 2008.

[23] S. Visacro and F. H. Silveira, "The impact of the frequency dependence of soil parameters on the lightning performance of transmission lines," *IEEE Trans. Electromagn. Compat.*, vol. 57, no. 3, pp. 434–441, Jun. 2015.

[24] S. Visacro and F. H. Silveira, "Lightning performance of transmission lines: Requirements of tower-footing electrodes consisting of long counterpoise wires," *IEEE Trans. Power Del.*, vol. 31, no. 4, pp. 1524–1532, Aug. 2016.

[25] M. A. O. Schroeder, M. T. Correia de Barros, A. C. S. Lima, M. M. Afonso, and R. A. R. Moura, "Evaluation of the impact of different frequency dependent soil models on lightning overvoltages," *Elect. Power Syst. Res.*, vol. 159, pp. 40–49, Jun. 2018.

[26] F. Vasconcellos, R. Alipio, and F. Moreira, "The influence of the frequency-dependent behavior of ground electrical parameters on the lightning performance of transmission lines," in *Proc. IEEE Int. Conf. Ind. Appl.*, 2021, pp. 1408–1414.

[27] Z. G. Datsios, P. N. Mikropoulos, and T. E. Tsovilis, "Closed-form expressions for the estimation of the minimum backflashover current of overhead transmission lines," *IEEE Trans. Power Del.*, vol. 36, no. 2, pp. 522–532, Apr. 2021.

[28] Z. G. Datsios, D. G. Patsalis, P. N. Mikropoulos, and T. E. Tsovilis, "Effects of approximating recorded lightning currents with CIGRE waveforms on computed fast-front overvoltages and critical lightning currents causing flashover to overhead transmission lines," *IEEE Trans. Power Del.*, vol. 38, no. 5, pp. 3084–3094, Oct. 2023.

[29] "Guide to procedures for estimating the lightning performance of transmission lines," CIGRE Working Group 33.01, Tech. Brochure 63, Oct. 1991.

[30] "Procedures for estimating the lightning performance of transmission lines – New aspects," CIGRE Working Group C4.23, Tech. Brochure 839, Jun. 2021.

[31] Z. G. Datsios, P. N. Mikropoulos, T. E. Tsovilis, and S. I. Angelakidou, "Estimation of the minimum backflashover current of overhead lines of the Hellenic transmission system through ATP-EMTP simulations," in *Proc. Int. Colloq. Lightning Power Syst.*, 2016, pp. 1–11.

[32] Z. G. Datsios, P. N. Mikropoulos, and T. E. Tsovilis, "Effects of lightning channel equivalent impedance on lightning performance of overhead transmission lines," *IEEE Trans. Electromagn. Compat.*, vol. 61, no. 3, pp. 623–630, Jun. 2019.

[33] J. R. Marti, "Accurate modelling of frequency-dependent transmission lines in electromagnetic transient simulations," *IEEE Trans. Power App. Syst.*, vol. PAS-101, no. 1, pp. 147–157, Jan. 1982.

[34] M. A. Sargent and M. Darveniza, "Tower surge impedance," *IEEE Trans. Power App. Syst.*, vol. PAS-88, no. 5, pp. 680–687, May 1969.

[35] IEEE WG on Lightning Performance of TL, "A simplified method for estimating lightning performance of transmission lines," *IEEE Trans. Power App. Syst.*, vol. PAS-104, no. 4, pp. 919–932, Jul. 1985.

[36] Z. G. Datsios and P. N. Mikropoulos, "Implementation of leader development models in ATP-EMTP using a type-94 circuit component," in *Proc. 32nd Int. Conf. Lightning Protection*, 2014, pp. 735–741.

[37] Z. G. Datsios and P. N. Mikropoulos, "Modeling of lightning impulse behavior of long air gaps and insulators including predischarge current: Implications on insulation coordination of overhead transmission lines and substations," *Elect. Power Syst. Res.*, vol. 139, pp. 37–46, Oct. 2016.

[38] C. L. Longmire and K. S. Smith, "A universal impedance for soils," DNA 3788T, Mission Research Corp., Santa Barbara, CA, Oct. 1975.

[39] K. Berger, "Novel observations on lightning discharges: Results of research on Mount San Salvatore," *J. Franklin Inst.*, vol. 283, no. 6, pp. 478–525, Jun. 1967.

[40] T. Narita, T. Yamada, A. Mochizuki, E. Zaima, and M. Ishii, "Observation of current waveshapes of lightning strokes on transmission towers," *IEEE Trans. Power Del.*, vol. 15, no. 1, pp. 429–435, Jan. 2000.

[41] L. Dubé, *MODELS in ATP, Language Manual*, 1996.

[42] L. Dubé, *Users' Guide to MODELS in ATP*, 1996.

[43] H. Motoyama, K. Shinjo, Y. Matsumoto, and N. Itamoto, "Observation and analysis of multiphase back flashover on the Okushishiku test transmission ine caused by winter lightning," *IEEE Trans. Power Del.*, vol. 13, no. 4, pp. 1391–1398, Oct. 1998.

[44] Z. X. Li and J. C. Wei, "Numerical simulation grounding system buried within horizontal multilayer Earth in frequency domain," *Commun. Numer. Methods Eng.*, vol. 23, no. 1, pp. 11–27, Jan. 2007.

[45] H. K. Høidalen, L. Prikler, and F. Peñaloza, *ATPDraw Version 7.0 for Windows Users' Manual*. Trondheim, Norway: NTNU, 2019.

[46] Z. G. Datsios, P. N. Mikropoulos, and T. E. Tsovilis, "Impulse resistance of concentrated tower grounding systems simulated by an ATPDraw object," in *Proc. Int. Conf. Power Syst. Trans.*, 2011, pp. 1–5.

[47] Z. G. Datsios, P. N. Mikropoulos, T. E. Tsovilis, and S. I. Angelakidou, "Effect of concentrated tower grounding system modeling on the minimum backflashover current and BFR of 150 and 400 kV overhead transmission lines," in *Proc. IEEE Int. Conf. High Voltage Eng. Appl.*, 2018, pp. 1–4.

[48] *IEEE Guide for Improving the Lightning Performance of Transmission Lines*, IEEE Standard 1243-1997, 1997.

[49] P. Chowdhuri et al., "Parameters of lightning strokes: A review," *IEEE Trans. Power Del.*, vol. 20, no. 1, pp. 346–358, Jan. 2005.

[50] F. H. Silveira and S. Visacro, "Lightning parameters of a tropical region for engineering application: Statistics of 51 flashes measured at Morro do cachimbo and expressions for peak current distributions," *IEEE Trans. Electromagn. Compat.*, vol. 62, no. 4, pp. 1186–1191, Aug. 2020.

[51] M. Nicora, D. Mestriner, M. Brignone, M. Bernardi, R. Procopio, and E. Fiori, "A 10-year study on the lightning activity in Italy using data from the SIRF network," *Atmos. Res.*, vol. 256, 2021, Art. no. 105552.

[52] Z. G. Datsios, P. N. Mikropoulos, and T. E. Tsovilis, "Evaluation of the backflashover performance of a 150 kV overhead transmission line as affected by lightning attachment models and peak current distributions," in *Proc. Int. Conf. Ground. Lightning Phys. Effects*, 2023, pp. 238–243.